



Simulation Science Laboratory 2018

An Analysis Tool for Materials Design

Students:

Praneeth Katta Venkatesh Babu
Christian Partmann
Johannes Wasmer

Supervisors:

Stefan Blügel PROF. DR.
Stefan Rost MSc
Quantum Theory of Materials PGI-1
Forschungszentrum Jülich

Abstract — Lorem ipsum dolor sit amet, consectetur adipiscing elit. Sed non risus. Suspendisse lectus tortor, dignissim sit amet, adipiscing nec, ultricies sed, dolor. Cras elementum ultrices diam. Maecenas ligula massa, varius a, semper congue, euismod non, mi. Proin porttitor, orci nec nonummy molestie, enim est eleifend mi, non fermentum diam nisl sit amet erat. Duis semper. Duis arcu massa, scelerisque vitae, consequat in, pretium a, enim. Pellentesque congue. Ut in risus volutpat libero pharetra tempor. Cras vestibulum bibendum augue. Praesent egestas leo in pede. Praesent blandit odio eu enim. Pellentesque sed dui ut augue blandit sodales. Vestibulum ante ipsum primis in faucibus orci luctus et ultrices posuere cubilia Curae; Aliquam nibh. Mauris ac mauris sed pede pellentesque fermentum. Maecenas adipiscing ante non diam sodales hendrerit. Ut velit mauris, egestas sed, gravida nec, ornare ut, mi. Aenean ut orci vel massa suscipit pulvinar. Nulla sollicitudin. Fusce varius, ligula non tempus aliquam, nunc turpis ullamcorper nibh, in tempus sapien eros vitae ligula. Pellentesque rhoncus nunc et augue. Integer id felis.

Keywords Lorem ipsum dolor sit amet, consectetur adipiscing elit. Sed non risus. Suspendisse lectus tortor.

AICES
Schinkelstr. 2
Rogowski Building
4th Floor
52062 Aachen

Acknowledgments

Lorem ipsum dolor sit amet, consectetur adipiscing elit. Sed non risus. Suspendisse lectus tortor, dignissim sit amet, adipiscing nec, ultricies sed, dolor. Cras elementum ultrices diam. Maecenas ligula massa, varius a, semper congue, euismod non, mi. Proin porttitor, orci nec nonummy molestie, enim est eleifend mi, non fermentum diam nisl sit amet erat. Duis semper. Duis arcu massa, scelerisque vitae, consequat in, pretium a, enim. Pellentesque congue. Ut in risus volutpat libero pharetra tempor. Cras vestibulum bibendum augue. Praesent egestas leo in pede. Praesent blandit odio eu enim. Pellentesque sed dui ut augue blandit sodales. Vestibulum ante ipsum primis in faucibus orci luctus et ultrices posuere cubilia Curae; Aliquam nibh. Mauris ac mauris sed pede pellentesque fermentum. Maecenas adipiscing ante non diam sodales hendrerit. Ut velit mauris, egestas sed, gravida nec, ornare ut, mi. Aenean ut orci vel massa suscipit pulvinar. Nulla sollicitudin. Fusce varius, ligula non tempus aliquam, nunc turpis ullamcorper nibh, in tempus sapien eros vitae ligula. Pellentesque rhoncus nunc et augue. Integer id felis.

Contents

1	Introduction	1
2	Theoretical Background	3
3	Implementation	5
3.1	HDF Preprocessor Module	5
3.1.1	Interface	5
3.1.2	Implementation for Band Structure Visualization	8
3.2	Visualization Module & Interactive Graphical Frontends	8
3.2.1	Visualization Module	8
3.2.2	Desktop Frontend	9
3.2.3	Web Frontend	9
4	Manuals	11
4.1	User Manual	11
4.1.1	System Requirements & Installation	11
4.1.2	Input Data Formats	11
4.1.3	GUI Usage	11
4.1.4	Troubleshooting	11
4.2	Developer Manual	11
4.2.1	Extending the Preprocessor	11
4.2.2	Extending the Visualization & Frontends	11
5	Applications	13

5.1	Web Frontend: MoSe_2 Crystal	13
5.2	Desktop Frontend: Co Crystal	15
5.3	Derived physical Quantities: Differentiation	15
5.3.1	Differentiation	16
6	Conclusion	19
6.1	Outlook	19

List of Figures

2.1	Brillouin zone of a fcc lattice. The red curve in the reciprocal lattice represents a possible sampling path of $E(k)$ in the reciprocal lattice.	4
3.1	Module Design	6
3.2	The preprocessor module.	7
3.3	Band Unfolding	8
3.4	Visualization Module Design	9
5.1	Atom Plot of a $MoSe_2$ monolayer	13
5.2	Bandstructure of a $MoSe_2$ crystal	14
5.3	Bandstructure of a $MoSe_2$ monolayer	14
5.4	Bandstructure of a $MoSe_2$ monolayer without unfolding weights	15
5.5	Comparison between FFT differentiation method and central finite difference method	17

List of Abbreviations

Chapter 1

Introduction

Chapter 2

Theoretical Background

...some introduction sentence depending on into chapter...

Fleur computes the electronic structure in crystals using the Density Functional Theory approach (DFT), which is the state of the art method for this problem. The many-body Schrödinger equation, that can be used to describe electrons in solids, is almost impossible to solve directly, because the storage of the wavefunctions of each of the N electrons in the system at each spatial coordinate exceeds the memory of any currently available computer for even quite small N . This motivates the DFT approach, that uses two fundamental theorems to reduce the computational complexity of the many-body problem significantly: The Hohenberg-Kohn theorem allows to use the electron density instead of the N -electron wavefunctions to uniquely characterize the ground state of a system. With the Kohn-Sham equations, the interacting Hamiltonian of the system can be replaced by non-interacting equations with an effective potential. This approach reduces the dimensionality of the problem from N^3 to 3 and trades the interacting Hamiltonian for a set of non-interacting equations that have to be solved self-consistently. In general, the DFT approach is not just limited to computations of electrons in crystals, but is also for example used in chemistry to compute nonperiodic molecules. The output of a DFT calculation includes various physical quantities (for example the 3-dimensional spatial electron density, which is the central quantity in DFT calculations), but for this project we focus on two quantities that are easy to interpret, already reduced in dimensionality and frequently used in both experimental and theoretical physics.

The band structure $E(\vec{k})$ represents the eigenenergies of the eigenfunctions of the Hamiltonian for each crystal momentum \vec{k} . It is the dispersion relation of electrons in the crystal and relates allowed momenta and energies. In general, $E(\vec{k})$ is defined at any point inside the Brillouin zone, which is a special choice of the unit cell in the reciprocal lattice of the crystal. Both, the real-space lattice and the reciprocal lattice are shown for a face centered cubic (fcc) crystal in figure 2.1. For larger unit cells with fewer symmetries, the Brillouin zone can be much more complicated than in the shown example. In order to reduce the dimensionality of

$E(\vec{k})$ with $k \in \mathbb{R}^3$, the dispersion relation is only sampled along a discrete one-dimensional path between high symmetry points in the Brillouin zone. This path still contains most of the relevant physical features.

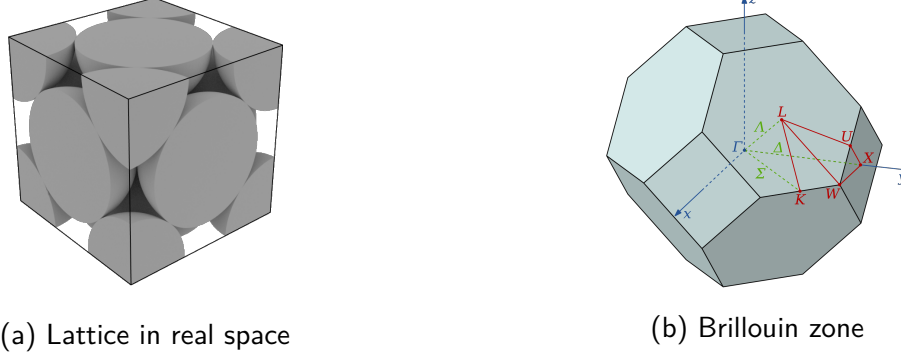


Figure 2.1: Brillouin zone of a fcc lattice. The red curve in the reciprocal lattice represents a possible sampling path of $E(k)$ in the reciprocal lattice.

The second central quantity in this project is the Density of States (DOS) $D(E)$, which describes the number of states per energy interval that is independent from the crystal momentum. In this sense, the DOS is also derived from $E(\vec{k})$, but instead of just selecting a subset, the \vec{k} dependency is summed out. Both complementary quantities together are a common choice for comprehensive visualizations of electronic structure data while still capturing most of the important physics.

For applications, it is useful to investigate where the contributions to $E(k)$ and $D(E)$ come from. Therefore, the data contains the weights of each basis function of the DFT calculation belonging to the individual atom groups and the orbitals. This means, spatial information about the system can be restored by considering only contributions from certain atom groups. (An atom group contains all atoms that are equivalent with respect to symmetries of the real space lattice.) On the other hand, the projection on the hydrogen orbitals s, p, d, f encode information about the shape of the wavefunction at each atom. These contributions are stored in the form of relative weights that can be summed to include contributions for multiple groups and orbitals. In case of distinct spins in the crystal, $E(k)$, $D(E)$ and the weights can be different for both spins and are therefore stored individually.

Chapter 3

Implementation

As per the requirements expounded upon in the introduction, the deliverable of the project should be a finished software product. The software is written in Python so as to integrate easily with the research group's ongoing software projects around the Fleur code [Blü+18]. These are chiefly the group's materials science tool collection `masci-tools` [RBR18], where also this project's code is hosted, and the 'Automated Interactive Infrastructure and Database for Computational Science' (AiiDA) [Piz+16]. The product stakeholders split into frontend users and code developers. In order to accommodate this, the product is organized into three unidirectionally dependent subpackages or -modules, see Figure 5.1.

An important design consideration was to account for unknown use cases. This has been realized in each submodule by the decoupling of **interface** and **implementation**. The interfaces do not rely on any specific input file format, visualization method or package, unlike the implementations for a specific task or **application**. The word 'application' in this section denotes the band structure and density of states visualization, and for these, implementations are provided.

This design choice was also one reason why the product does not reuse any of the `masci-tools` routines which partly solve quite similar problems, but seemed to be too specialized in an cursory code review. For these developers, one added value of the project product could be to inspire the hopefully easy integration into a common interface, where the current abstraction level could serve as a starting point.

3.1 HDF Preprocessor Module

3.1.1 Interface

This is the 'backend' of the tool. It is basically a file reader for the input data, for example a Fleur simulation output. Supported formats are the Hierarchical Data Format (HDF) [Kor11] for the band structure, and a simple Fleur-specific comma-separated values (CSV) format for the density of states (DOS).

The HDF format is basically a binary flexible container for all kinds of common binary and text file formats, each of which constitutes a Dataset inside the HDF file. The format supports metadata annotation and high-throughput input/output (I/O). As a consequence, it is considered by some developers in some application domains relying on numerical simulation codes, to be one possible base for the establishment of common domain-specific rich data exchange standards in order to increase code interoperability. These developers are in the process of extending their codes' I/O capabilities towards that end. However, HDF's flexibility comes at the price of a relatively complex Application Programming Interface (API) as the keyhole for all operations.

The preprocessor module tries to hide that complexity by offering the Recipes interface, see Figure 3.2. A specific application Recipe is a dictionary that aims to describe a complete [Extract-Transform-Load](#) (ETL) pipeline for one specific application. The 'extract' is the reading of a dataset from HDF, the 'transform' a sequence of once-through functions applied to the the dataset, and the 'load' the aggregation of all transformed datasets into one runtime object that has all the methods for operations on the data that are going to be used later on in the intended application.

The 'transform' and 'output' type methods are defined in hierarchical Transform and Output_Type classes, which sort them from general to application-specific applicability. This structure is built using Python's AbstractBaseClass (ABC) interface and multiple inheritance. The advantages of the 'Recipes approach' are:

- All ETL processes for one application are collected in one simple list (the recipe), not locked in different code locations with conflicting contexts. In this list, entries can be sorted in any manner, e.g. alphabetical for perusal.
- Recipes are de/serializable (can be read from and saved to disk) and thus be created and manipulated by code.
- The ETL processes declared in this way can be easily reused across applications. A recipe

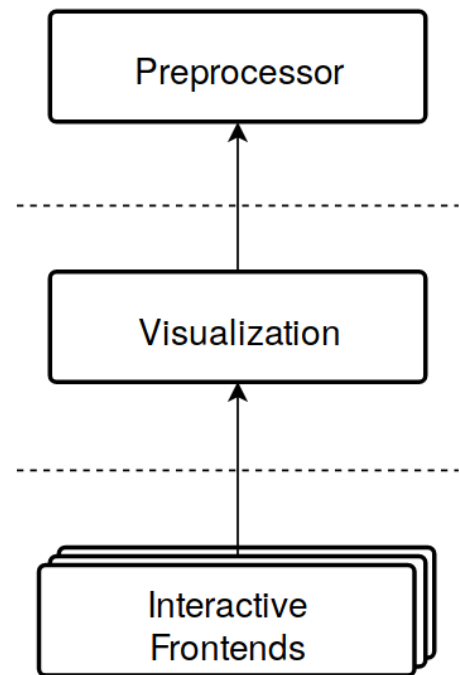


Figure 3.1: Module Design

can combine different output types into a new type.

The feature that enables this flexibility is **type introspection**: the preprocessor processes the datasets listed in the recipe in the order of their mutual dependencies as found in the used transform and output methods. When all transformed datasets have been added to the object, all specified output types are searched and all their methods and attributes added. Thus the output object's type is defined at runtime, when the preprocessing is finished.

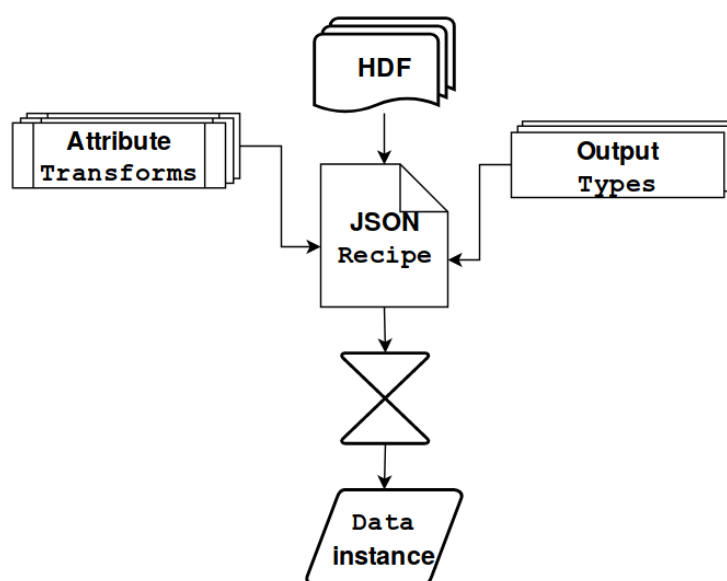


Figure 3.2: The preprocessor module.

Listing 3.1: Recipe FleurBands excerpt: dataset BravaisMatrix

```

1  "bravaisMatrix": {
    "h5path": "/cell/bravaisMatrix",
    "description": f"Coordinate_transformation_internal_to_physical
    ↪_for_atoms",
    "transforms": ['Transform.move_to_memory',
                   [Transform.scale_with_constant, "bohr_radius", "
    ↪angstrom"]]
6  },captionpos

```

3.1.2 Implementation for Band Structure Visualization

$$W_{s,k,\nu}^{\text{eff}} = \left(\frac{\sum_{\substack{g \in \text{groups} \\ l \in \text{characters}}} n_{s,k,\nu,g,l} N_g}{\sum_{\substack{g \in \text{all groups} \\ l \in \text{all characters}}} n_{s,k,\nu,g,l} N_g} \right) \left(W_{s,k,\nu}^{\text{unf}} \right)^\alpha \quad (3.1)$$

$W_{s,k,\nu}^{\text{eff}}$ is the effective weight. The indices denote: s spin, k point on k -path, ν band, g group, l character. $n_{s,k,\nu,g,l}$ is the state-specific l -like charge. N_g denotes the number of atoms in a group. $W_{s,k,\nu}^{\text{unf}}$ is the unfolding weight and α its exponent.

Calculations can be done with a crystal unit cell (UC) or a super cell

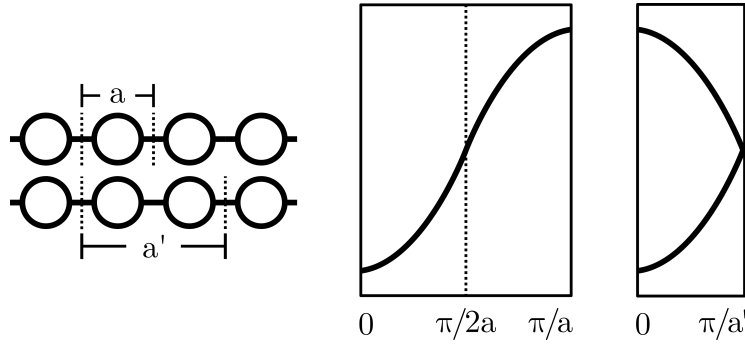


Figure 3.3: Band Unfolding: Example for a simple monatomic chain [Hof87].

TODO describe how bandstructure data is preprocessed for visualization including user selections AND optimizations

3.2 Visualization Module & Interactive Graphical Frontends

TODO Frontends: combine into one subsection when finished. usage will be in user manual next section.

3.2.1 Visualization Module

The Python visualization landscape abounds with a rapidly evolving plethora of plotting libraries for different application contexts and technology stacks [VR17]. Thus the project's visualization module first design objective was to account for that by decoupling from specific library use, and modularizing applications. This structure again is built using Python's `AbstractBaseClass`

(ABC) interface and multiple inheritance. Each application is represented by an abstract base class that contains the common plotting method signatures. Each plotting library is represented by an abstract base class that contains library-specifics. An implementation inherits both from one library base class and one or more application base classes. See Fig. 3.4 for an impression. Thus switching the library in a frontend should require minimal adjustment, and a new application can be build using existing ones.

The second design objective was for the plotting methods to to hide all interactions with the actual plotting library used under the hood, while the method arguments only relate to the preprocessed data being plotted. Thus different frontend implementations only all call one common method for one specific plot and receive the identical visualization with identical interactive behavior.

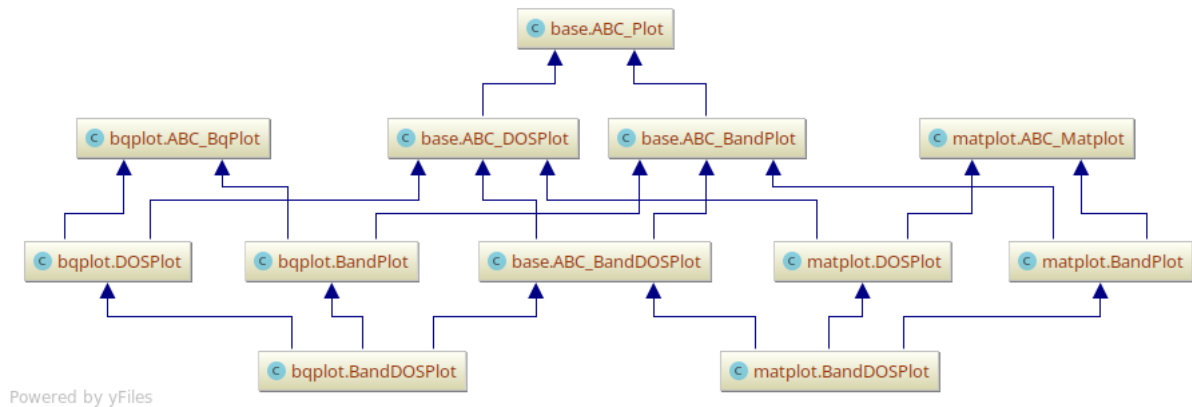


Figure 3.4: Visualization Module Design: Example Structure for two applications BandPlot and DOSPlot, and two plotting libraries matplotlib and bqplot.

3.2.2 Desktop Frontend

3.2.3 Web Frontend

As Web Frontends increasingly replace traditional Desktop Frontends in the modern software environment [Dou+08], so Python-based Frontends and visualizations are increasingly moving towards the browser. There, GUIs with interactive visualizations are often called **Dashboards**. In the project context, a survey was undertaken in order to choose the most suitable technology stack. The full survey is documented in [Was19]. The requirements for the solution stack, added to those in the introduction, were as follows:

1. **openness**: relies solely on Open-Source-Software (OSS) with licensing suitable for academic use, sports a stable release cycle, developer base and documentation,

2. **dashboarding**: features graphical control elements (widgets) that interact with InfoVis¹ plotting libraries,
3. **deployment**: ideally works like any web service, i.e. only a modern web browser is required to use it,
4. **maintenance**: requires only Python and no Web Development knowledge like e.g. Javascript, with respect to the product stakeholders.

The last point implies a client-server model where the dashboard app is hosted by a remote service. This model requires a communication framework and protocol between the Python interpreter running on the server and the JavaScript interpreter running in the client browser. As per requirement number two, unlike a generic Python web framework like e.g. [Flask](#), the framework should take care of that communication by itself. Four major frameworks were identified which fulfill the first three requirements: [Project Jupyter](#), [PyViz](#), [Bokeh](#), and [Dash by Plotly](#). The last two only partially fulfilled the last requirement, so they were discarded. PyViz is the newest contender among the four. Its expressed goal is to untangle the Python visualization jungle by providing one high-level API that ties together all major Python InfoVis libraries and data formats, including dashboarding. That ambitious goal comes at the price of sacrificing support for 3D plotting [[aut18](#)], which was needed in this project for the atoms plot. So PyViz had to be discarded.

That left Project Jupyter. By now, its widget library `ipywidgets` is integrated to work with a wide variety of popular plotting libraries. However, Jupyter only partially fulfills the third requirement – a Jupyter notebook (app) cannot, by itself, be published (deployed) as a stand-alone website outside a live Jupyter environment [[Bed18](#)]:

[...] “However, despite their web-based interactivity, the `ipywidgets`-based libraries (`ipyleaflet`, `pythreejs`, `ipyvolume`, `bqplot`) are difficult to deploy as public-facing apps because the Jupyter protocol allows arbitrary code execution” [...].

To avoid requiring users to setup a working Jupyter environment on their machine, the go-to solution for this problem is to setup a [JupyterHub](#) multi-user server. This still requires users to register an account there. Fortunately though, the intended users are contributors to the AiiDA project, and so should have access to the JupyterHub-based [AiiDaLab](#) service where the app can be registered. Details on this procedure and alternative hosting solutions can be found in the developer Section [4.2 on the facing page](#).

¹InfoVis libraries: visualizations of information in arbitrary spaces, not necessarily the three-dimensional physical world. Example: `matplotlib`. SciVis libraries: visualizing physically situated data. Example: VTK [[Bed18](#)].

Chapter 4

Manuals

4.1 User Manual

4.1.1 System Requirements & Installation

4.1.2 Input Data Formats

4.1.3 GUI Usage

The Desktop and Web Frontend are functionally identical and use the same graphical descriptors. Thus these points hold true for both alike.

Instead of dragging the sliders, values can be typed into their adjoining value displays as well.

TODO: web frontend: binder or colab link

4.1.4 Troubleshooting

4.2 Developer Manual

4.2.1 Extending the Preprocessor

4.2.2 Extending the Visualization & Frontends

TODO: publish on aidalab

TODO: hosting alternatives

- binder with example
- google colab (see jupy wiki or jupy awesome) [[Sch+18](#)]
- voila?

Chapter 5

Applications

To illustrate the use of the graphical user interface, two different physical applications are shown in the desktop and the web frontend, respectively. From the physics point of view, the example in the desktop version focuses more on the density of states and the visualization of spin contributions, while the dataset in web frontend focuses on the band structure $E(k)$ and the visualization of defect states in supercells.

5.1 Web Frontend: MoSe₂ Crystal

Figure 5.2 shows the visualization of a band structure calculation of a 3 dimensional Molybdenum diselenide (MoSe₂ bulk) crystal using the default settings of the GUI. Even with the default settings the band structure plots clearly indicate, that MoSe₂ is a semiconductor, since there are no states at the Fermi level. Because the minimum of the conduction band is located at an other k as the maximum of the valence band, the plot shows that MoSe₂ has an indirect band gap. This indicates that for the transition with the smallest energy difference between valence and the conduction band, both, energy and momentum have to change.

In contrast to the 3 dimensional extended MoSe₂ crystal, a MoSe₂ monolayer (see Fig. 5.3) has a direct band gap but is still a semiconductor. Furthermore, the MoSe₂ monolayer has a defect atom in every 9th unit cell and the DFT computation is therefore done in a 3×3 supercell to restore periodicity. This is the reason for the much greater number of states

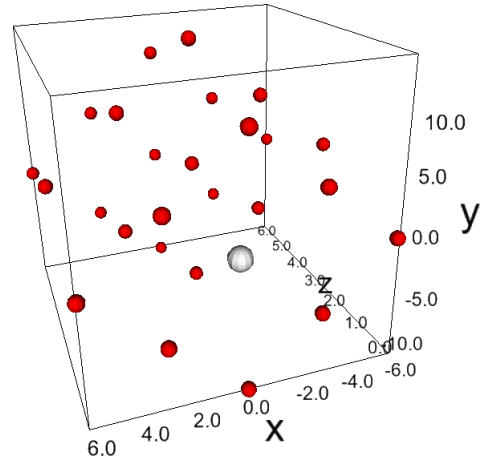


Figure 5.1: Atom Plot of a *MoSe₂* monolayer with the defect atom selected in the web frontend

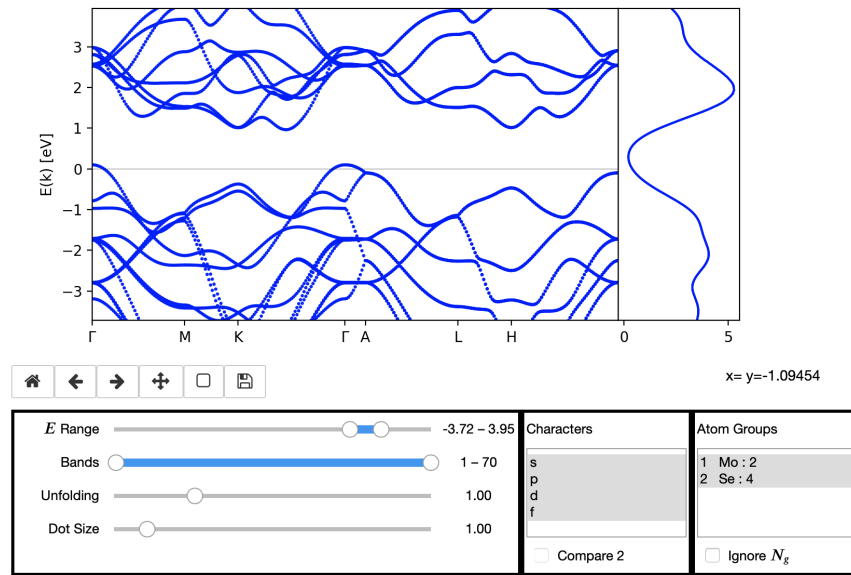


Figure 5.2: Bandstructure of a MoSe_2 crystal using the default settings of the web frontend

in the band structure plot.

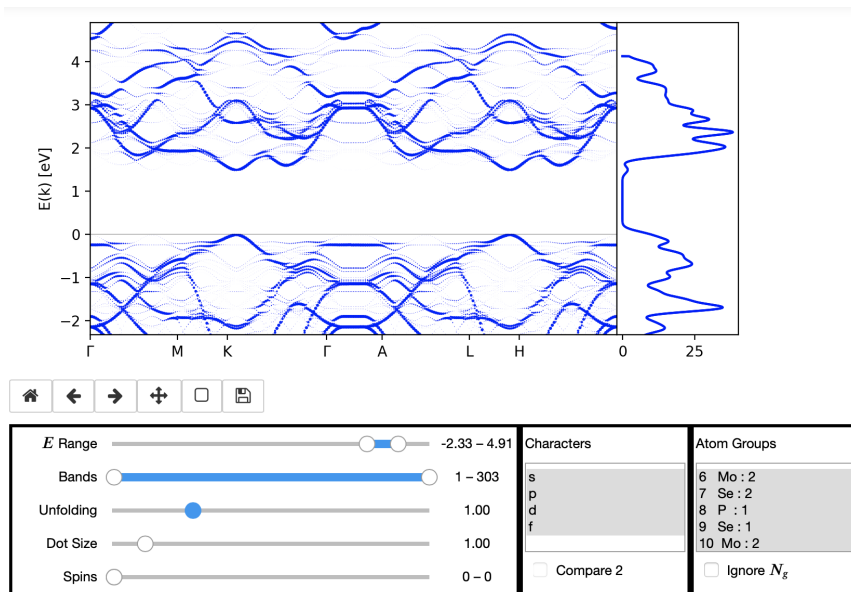


Figure 5.3: Bandstructure of a MoSe_2 monolayer using the default settings of the web frontend

Since the Brillouin zone of the supercell is smaller than the Brillouin zone of the same crystal without the defect, the supercell Brillouin zone is unfolded to the same size as the Brillouin zone of the unperturbed lattice. To account for the fact that the defect is only present in every 9th cell and its relative importance for the spectrum is therefore degraded, an unfolding weight is introduced to visualize the relative importance of bands in the unfolded Brillouin zone. By

default, the unfolding weight is used by our visualization tool, but it can gradually be turned off in order to highlight the impact of defect states. This is shown in figure 5.4. To even better visualize the defect state, it would also be possible to select the atom group belonging the defect atoms only. In this example, the analysis with reduced band unfolding shows, that there are many more direct band gaps origination from the defect state.

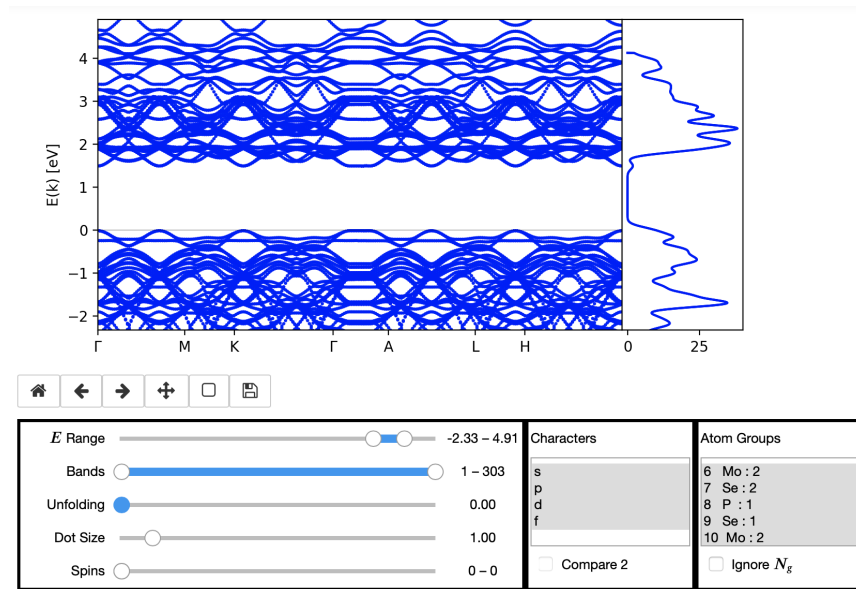


Figure 5.4: Bandstructure of a $MoSe_2$ monolayer without unfolding weights

5.2 Desktop Frontend: Co Crystal

5.3 Derived physical Quantities: Differentiation

The kind of datasets handled in the scope of the project did not lend themselves readily to applications of automatic differentiation techniques. Nevertheless, it is possible to derive meaningful physical quantities from the band structure using numerical differentiation techniques.

The effective mass m^* represents the mass, that an electron appears to have due to the inter-atomic forces in the crystal. At every \vec{k}_0 , where $E(\vec{k})$ has a local extremum, $E(\vec{k})$ can be expanded in a Taylor series with a vanishing first order term $E(\vec{k}) = E_0 + \frac{\partial E(\vec{k})}{\partial \vec{k}} \cdot (\vec{k} - \vec{k}_0)^2$. Comparing this to the dispersion relation of a free electron $E(\vec{k})_{free} = \frac{\hbar^2 \vec{k}^2}{2m_e}$ motivates the

general definition

$$m_{k_i, k_j}^* = \hbar^2 \left(\frac{\partial^2 E(\vec{k})}{\partial k_i \partial k_j} \right)^{-1} \quad (5.1)$$

Since $\frac{\partial^2 E(\vec{k})}{\partial k_i \partial k_j}$ depends on the direction of the partial derivatives, m_{k_i, k_j}^* is a tensor. Because the band structure files only contain a discrete sampled path in the Brillouin zone, only the derivatives that correspond to the direction from one high-symmetry point to the next can be computed. We are only interested in the diagonal terms of $m^*|_{i,j}$.

A second potentially interesting quantity is the group velocity $v_G(\vec{k})$ associated to each band. The group velocity $v_G(\vec{k})$ at the Fermi energy $E = E_F$ is called Fermi velocity.

$$v_G(\vec{k})_{k_i} = \frac{1}{\hbar} \frac{\partial E(\vec{k})}{\partial k_i} \quad (5.2)$$

5.3.1 Differentiation

Since the k-mesh in DFT calculations is potentially very sparse, low order finite difference schemes are not expected to work well. Alternatively, one way to exploit all data points efficiently is to use fast Fourier transform methods, which are equivalent to the derivation of a truncated Fourier series. This method is expected to be well-suited for the problem since the graph of the band structure $(k, E(|k|))$ with $k \in \{-\Gamma, \dots, H, \dots, \Gamma\}$ is periodic, where Γ and H are arbitrary representatives of the high symmetry points. This periodicity in the reciprocal space is a direct consequence of the periodicity of the crystal.

In Fourier space, spatial derivatives transform into multiplications, which can easily be shown by partial integration.

$$f^{(n)}(x) = \mathcal{F}^{-1}((ik)^n \mathcal{F}(f(x))) \quad (5.3)$$

To test the FFT differentiation method, a band was selected that did not have intersections with other bands within the interval between two high symmetry points and a stationary point at the high symmetry points. Then a resolution study was done to investigate the impact of the number of points within the interval.

The comparison between the FFT and a first-order central difference approximation of the second derivative (FD) is shown in Fig. 5.5, where different k-mesh resolutions are compared to a derivative that is almost fully converged. The comparison indicates that for small N, the error of the FFT method is significantly smaller than the error of the FD derivative. This is especially striking in the vicinity of the high symmetry points, where the error of the differentiation is

required to be small in order to get good approximations for m^* , which is only meaningful close to the high symmetry points.

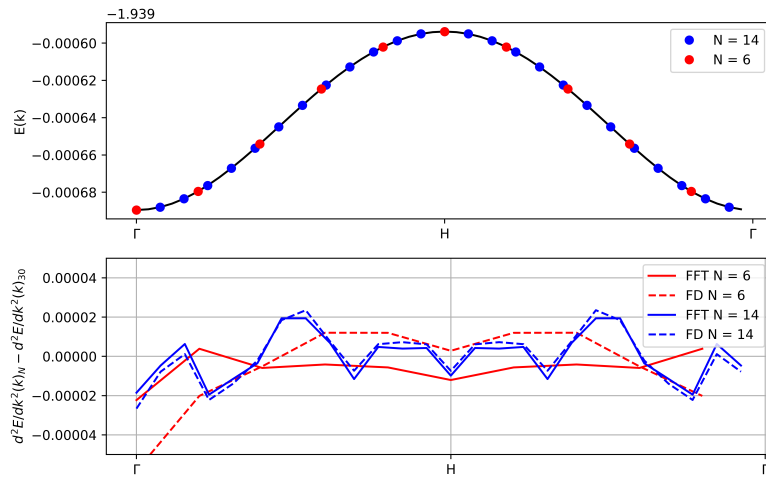


Figure 5.5: Comparison between FFT differentiation method and central finite difference method

When using more points, the difference between both approximation schemes is not significant. It is interesting to note, that the FFT method does not work anymore in the limit of extremely many points. In this case the derivative is dominated by Gibbs oscillations. These are most likely caused by small discontinuities in $E(k)$, due to basis changes inside the DFT computation.

At the current state the question remains to be answered whether the computation of m^* and v_g is useful. The number of bands, which the computation can be applied to is extremely limited. Since the bands in the data files are not labeled according to their corresponding eigenfunction but sorted by value, there are discontinuities at each point, where two bands intersect. This problem might be solved in the future.

Chapter 6

Conclusion

6.1 Outlook

TODO Module design:

- Preprocessor module: dataset dependencies for new recipes have to be explicitly stated. This could also be automatically resolved by type inspection.
- Frontends:
 - PyViz Param [\[Ste+19\]](#) makes it possible to decouple the formal description of a particular GUI from the GUI library used. This would serve to separate interface and implementation like it is done in the preprocessor and visualization submodules.

Bibliography

- [aut18] PyViz authors. *PyViz FAQ*. <http://pyviz.org/FAQ.html>. PyViz team. 2018.
- [Bed18] James Bednar. *Python Data Visualization 2018*. Blog. <https://www.anaconda.com/python-data-visualization-2018-why-so-many-libraries/> and <https://www.anaconda.com/python-data-visualization-2018-moving-toward-convergence/> and <https://www.anaconda.com/python-data-visualization-2018-where-do-we-go-from-here/>. 2018.
- [Blü+18] Stefan Blügel et al. *Fleur: full potential linearized augmented planewave code*. <http://www.judft.de>. 2018.
- [Dou+08] John R Douceur et al. “Leveraging Legacy Code to Deploy Desktop Applications on the Web.” In: *OSDI*. Vol. 8. 2008, pp. 339–354.
- [Hof87] Roald Hoffmann. “How chemistry and physics meet in the solid state”. In: *Angewandte Chemie International Edition in English* 26.9 (1987), pp. 846–878.
- [Kor11] Sandeep Koranne. “Hierarchical Data Format 5 : HDF5”. In: *Handbook of Open Source Tools*. Boston, MA: Springer US, 2011, pp. 191–200. ISBN: 978-1-4419-7719-9. DOI: [10.1007/978-1-4419-7719-9_10](https://doi.org/10.1007/978-1-4419-7719-9_10). URL: https://doi.org/10.1007/978-1-4419-7719-9_10.
- [Piz+16] Giovanni Pizzi et al. “AiiDA: automated interactive infrastructure and database for computational science”. In: *Computational Materials Science* 111 (2016), pp. 218–230. ISSN: 0927-0256. DOI: <https://doi.org/10.1016/j.commatsci.2015.09.013>. URL: <http://www.sciencedirect.com/science/article/pii/S0927025615005820>.
- [RBR18] Philipp Rüßmann, Jens Bröder, and Stefan Rost. *masci-tools*. <https://github.com/JuDFtTeam/masci-tools>. 2018.
- [Sch+18] Markus Schanta et al. *Awesome Jupyter*. <https://github.com/markusschanta/awesome-jupyter>. 2018.
- [Ste+19] Jean-Luc Stevens et al. *PyViz Param*. <https://github.com/pyviz/param>. 2019.

- [VR17] Jake VanderPlas and Nicolas Rougier. *Python Visualization Landscape*. <https://github.com/rougier/python-visualization-landscape>. 2017.
- [Was19] Johannes Wasmer. *Software Development Notes*. <https://github.com/Irratzo/notes>. 2019.